This PDF file includes

Supplemental data Text note 1

Figures S1 to S9

Supplementary note 1: case report

P is an Amerindian boy from Ecuador, with consanguineous parents. He was born in 2010. Both the pregnancy and the growth of the child were normal. P had a sister who presented persistent diarrhea from the age of four months and died from a severe respiratory infection at the age of six months. P1 presented gastroenteritis, otitis and respiratory infections since the age of six months, for which he was treated with several antibiotics. At eight months of age he was admitted to the intensive care unit (ICU) due to severe viral infection: flu A and B with pulmonary infiltrate; suspected bacterial superinfection, adenovirus and respiratory syncytial virus (RSV) infection, acute secondary respiratory failure, oral candidiasis and diaper dermatitis with *Candida albicans* superinfection.

Hypogammaglobulinemia was detected at the age of nine months and treated with intravenous immunoglobulin (IVIG), initially at a dose of 400 mg/kg doses every 3 weeks, but later on for some periods at 2 weeks intervals due poor maintenance of trough IgG levels.

At the age of thirteen months he suffered prolonged diarrhea due to *Campylobacter jejuni* infection. At eighteen months he presented again with prolonged diarrhea, without positive findings in the stools. Active chronic colitis was identified in a colon biopsy. Diarrhea persisted with occasional exacerbations and suspicion of bacterial overgrowth. At two years and 5 months, he was admitted to hospital with acute gastroenteritis due to adenovirus and a respiratory infection caused by RSV. Three

months later the patient was readmitted to hospital because of diarrhea due to adenovirus infection. Because of persistent diarrhoea, a colon biopsy was repeated and chronic non-specific colitis with moderated lymphocytic infiltration in *lamina propia* was observed. Coproculture and parasite tests were all negative. He was treated because of bacterial superinfection, severe malnutrition and ferropenic anemia, with mesalazine, oral metronidazole, and dietary modification, but the symptoms followed a fluctuating course. At the age of two years and 10 months, the patient was admitted to hospital for seizures and status epilepticus. Secondary diffuse leukoencephalopathy was diagnosed and the patient was treated with levetiracetam. PCR tests for pathogens, including enteroviruses, JC virus, BK, Parvovirus, Herpes family, were negative, and the course of the illness was favorable. During this episode neurological regression was observed, but progressively he recovered his normal basal status. At the age of three years and four months, the patient was admitted to the ward with diarrhea caused by *Clostridium difficile*, which was treated with oral vancomycin. After 24 hours was admitted to the ICU because of dizziness, disorientation and generalized weakness with focal abnormal movements. Suspected encephalitis of unknown etiology was observed. All microbiological cultures, PCR tests and autoimmune results were negative. The patient suffered severe neurological impairment without spontaneous respiratory pattern and eventually died due to respiratory failure.

The immunological studies at 9 months showed hypogammagloulinemia with moderately conserved IgM, without lymphopenia but reduced percentages of memory B and T cells. CD40L expression after stimulation, and CD3 and HLA Class I and II expression were normal. We sequenced the CD40, CD40 ligand (CD40L), uracil-DNA glycosylase (UNG), activation-induced cytidine deaminase (AID), and interleukin 2 receptor alpha (IL2R) genes; no mutations were found. The patient was suspected to

have a combined immunodeficiency based on the hypogammaglobulinemia with reduce memory B cells, and a possible cellular defect mainly expressed as maintain reduced memory T cells. Co-trimoxazole prophylaxis was recommended.

Supplementary figures

Figure S1

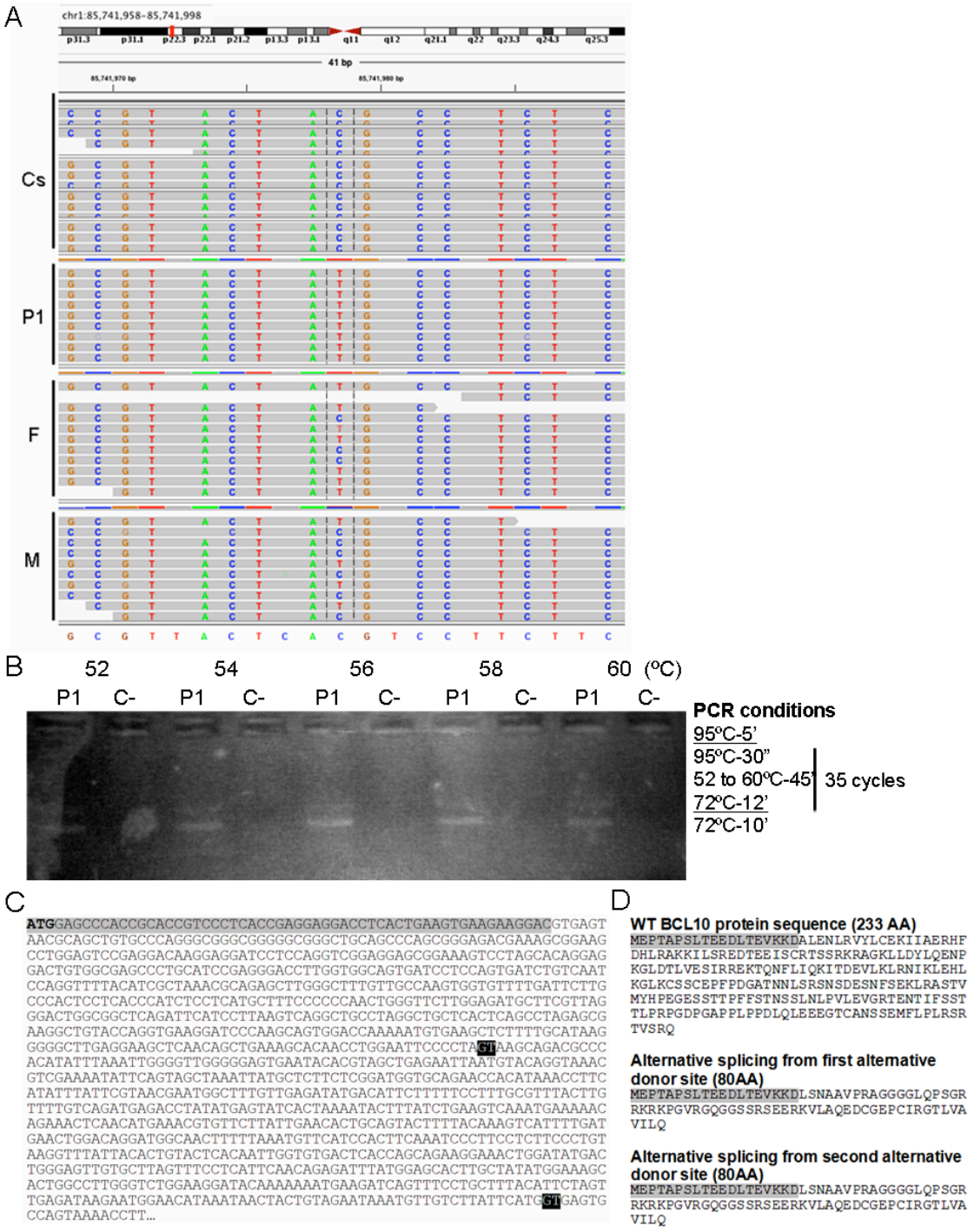

Figure S1. *BCL10* expression and alternative essential splicing in P1

(A) Illumina sequencing reads displayed for several controls (Cs), P1, his father (F) and his mother (M). Reads overlapping the mutation g.85741978C>T, homozygous in P1

and heterozygous in F and M. **(B)** PCR at different annealing temperatures, on cDNA from the HTLV-1 T cells of P1 and water (C-). Two bands were excised and the corresponding nucleic acids were inserted into the pcDNA™3.1 plasmid and sequenced. **(C)** Nucleotide sequence of exon 1, and part of intron 1 of human *BCL10*. Exon 1 is shown in gray, the ATG is shown in bold, and the two alternative donors generated by the *BCL10* mutation in P1 are shown as white words on a black background. The resulting two alternative mRNAs were detected by sequencing the plasmid after cloning. **(D)** Human WT BCL10 protein sequence and two potential transcript variants generated by alternative essential splicing. The protein sequence common to the products of the three cDNAs is shown in gray.

Figure S2

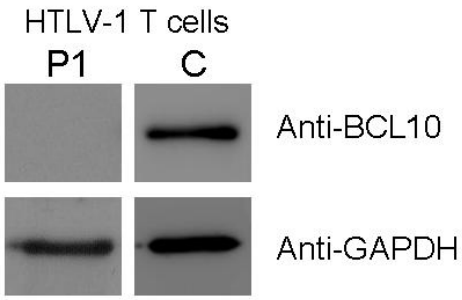

Figure S2. BCL10 levels in a patient with CID

Immunoblot analysis of BCL10 in HTLV-1 T cells from a control (C) and P1. GAPDH was used as a loading control. The panels illustrates results from a single experiment, representative of three carried out.

Figure S3.

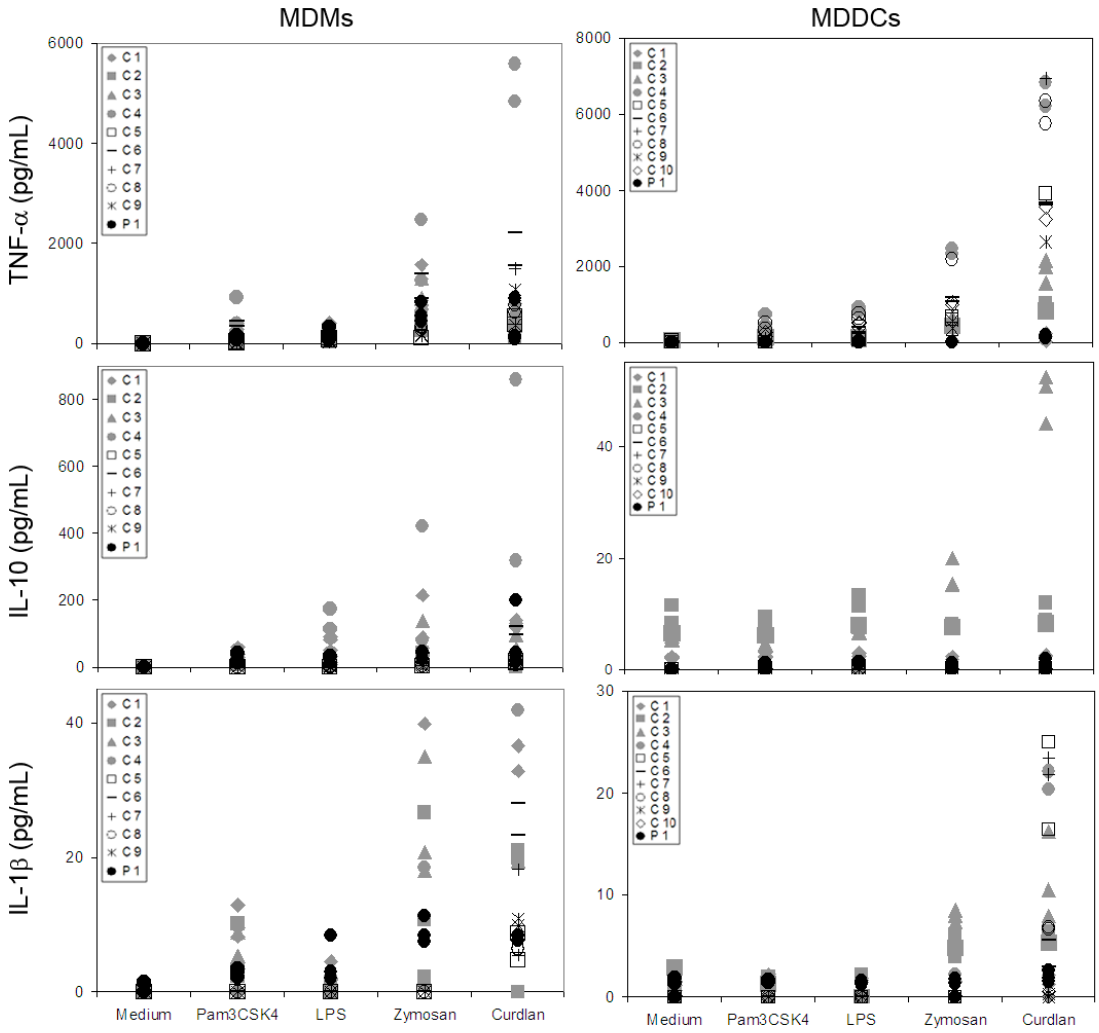

Figure S3. Production of cytokines by myeloid cells

The production of TNF-α, IL-10 and IL-1β in response to stimulation with Pam3CSK4, LPS, zymosan and curdlan, as assessed by CBA, in monocyte-derived macrophages (MDMs) and monocyte-derived dendritic cells (MDDCs). C1-C10 are positive controls and P1 is patient 1. Data are expressed as raw data from three independent experiments.

Figure S4

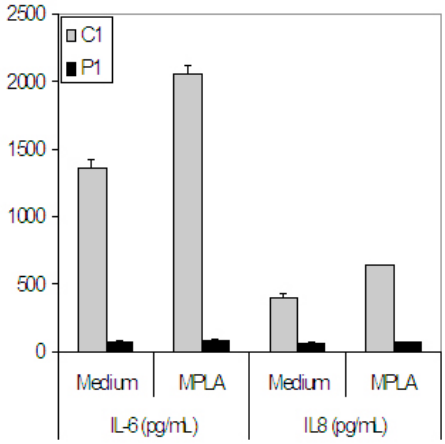

Figure S4. Impact of human BCL10 deficiency on fibroblast immunity

Production of IL-6 and IL-8, as assessed by CBA, in primary fibroblasts after stimulation with synthetic MPLA (a specific TLR4 agonist). C1 is the positive control. Values, (mean±SEM), were calculated from three independent experiments.

Figure S5

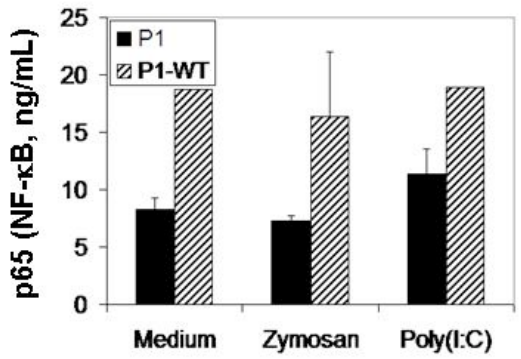

Figure S5. Impact of human BCL10 deficiency on fibroblast immunity. Complementation studies in fibroblasts.

NF-κB ELISA of nuclear extracts from fibroblasts from P1 and cells from P1 transfected with the BCL10-WT plasmid (P1-WT), after stimulation with Zymosan and Poly(I:C) for 60 min. Values, (mean±SEM), were calculated from three independent experiments.

Figure S6

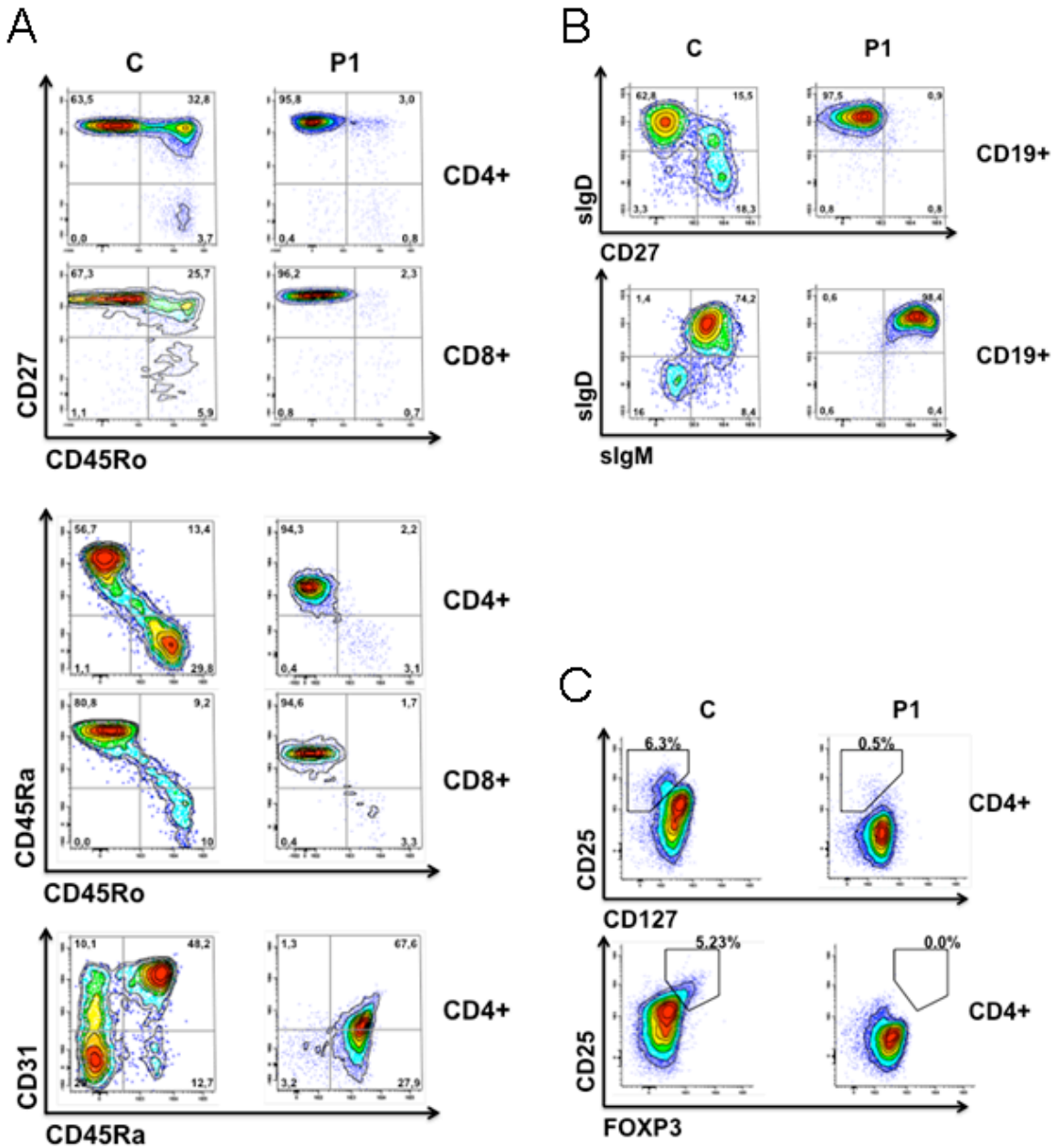

Figure S6. Strategy for the analysis of peripheral lymphocyte profiles by flow cytometry. (A) $CD4^+$ and $CD8^+$ gated as $CD3^+$ and based on the expression of CD27 and CD45RO, the CD4+ and CD8+ T-cell compartments were divided into naive, memory, memory effector and effector T cells. Recent thymic emigrants (RTEs) were identified on the basis of the expression of $CD31^+$ in naive T cells. **(B)** B-cell

subpopulations. Surface expression of immunoglobulins IgM and IgD and the expression of CD27 led to classification into three main subpopulations: $IgM^{+}IgD^{+}CD27^{-}$ naive B cells, $IgM^{+}IgD^{+}CD27^{+}$non-class-switched Memory B cells and $IgM^{-}IgD^{-}CD27^{+}$ class-switched memory B cells. **(C)** Regulatory T cells (Tregs) were detected on the basis of the expression of Foxp3 and in $CD4^{+}CD25^{+}CD127^{-}$ T lymphocytes. The percentages for each population are indicated in each quadrant.

Figure S7

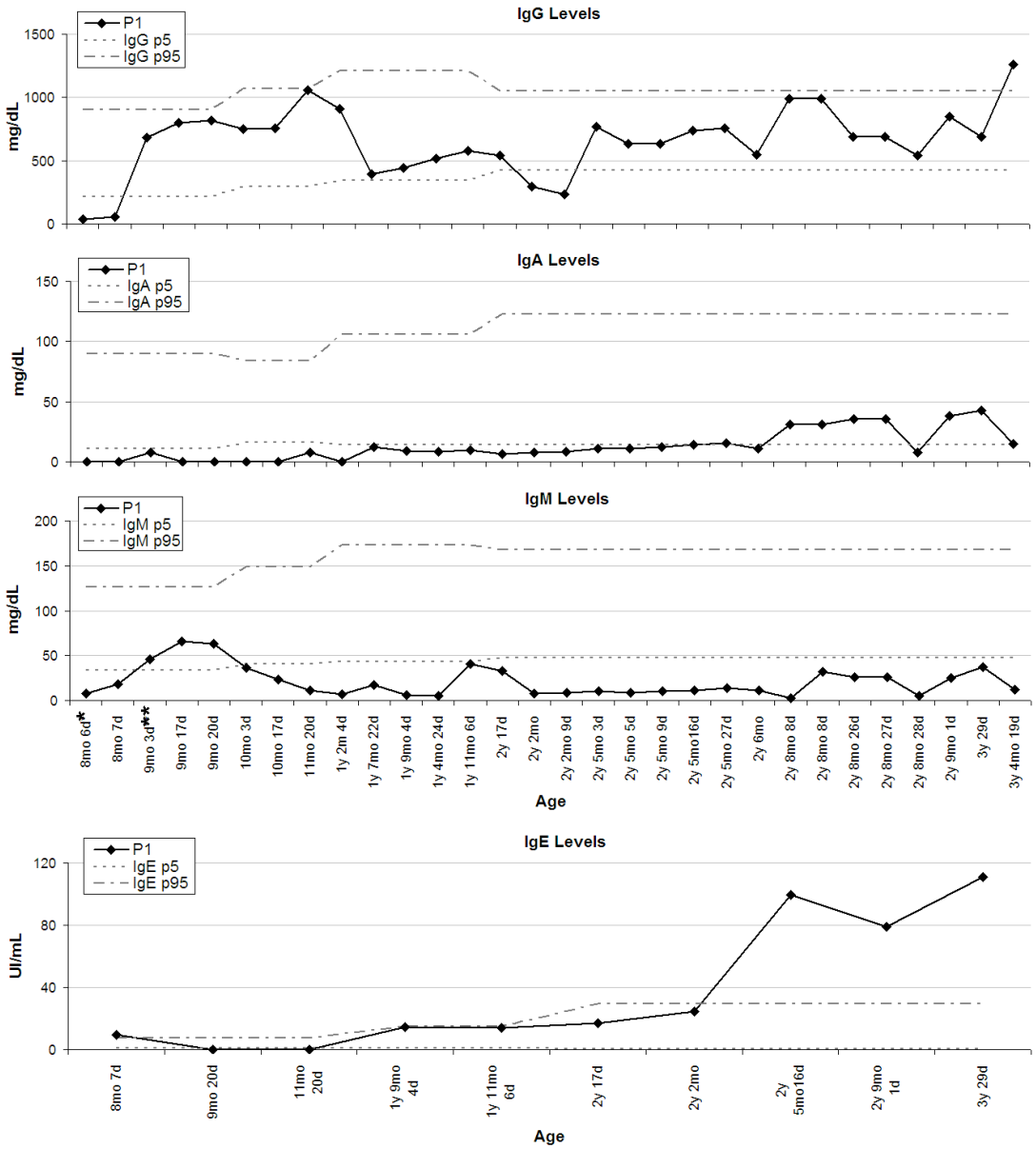

Figure S7. Immunoglobulin (Ig) levels

Change in Ig levels (IgG, IgA, IgM and IgE) with age measured by nephelometry for patient 1. * corresponds to the first hospitalization of P1. ** indicates the age at which IVIG treatment was initiated.

Figure S8

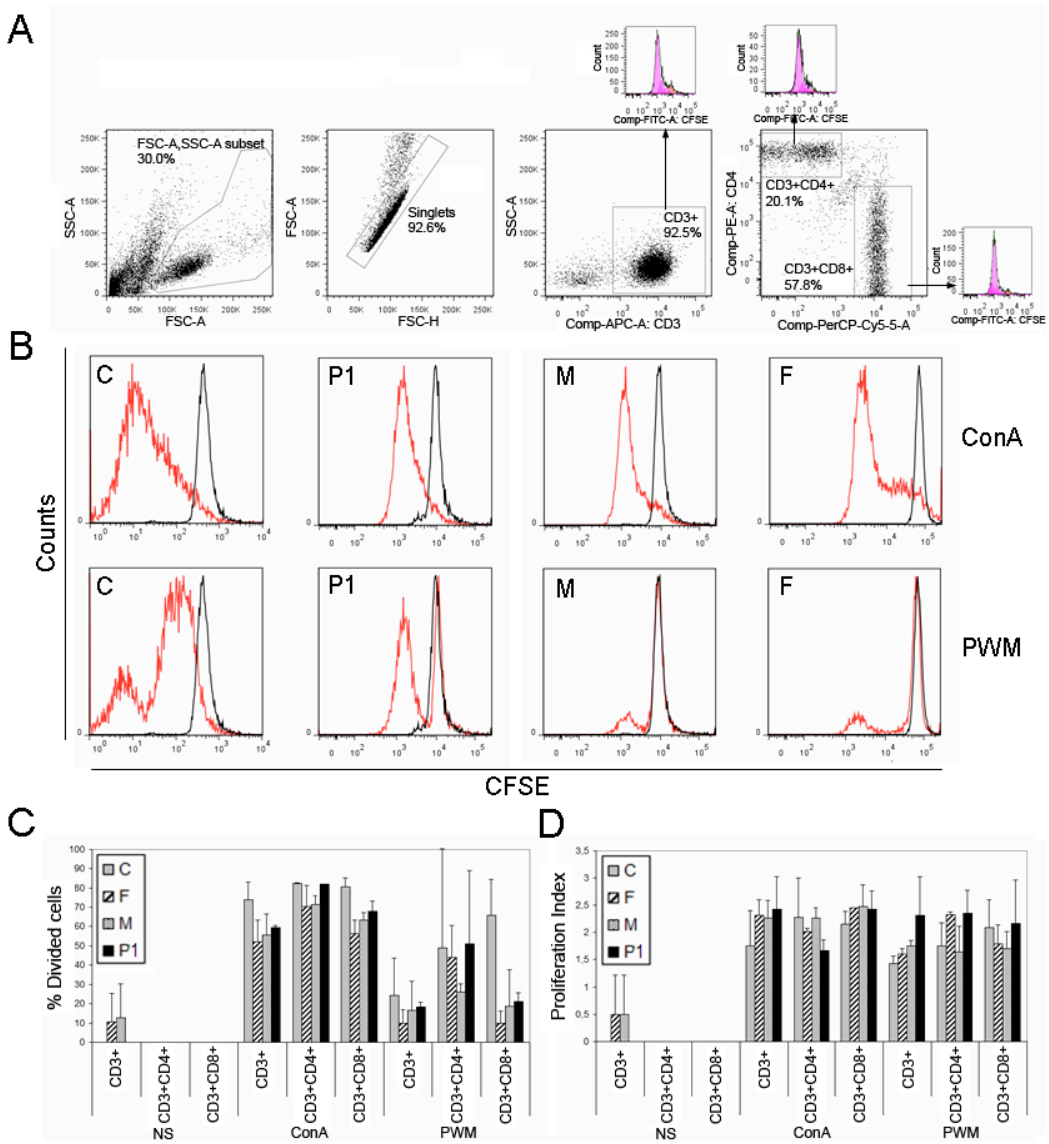

Figure S8. Proliferative response of T cells

(A) Sequential analysis of the proliferation of T-cell subpopulations with CFSE. FCS vs. SSC selection was applied and singlets were selected on the basis of their similar height (FSC-H) and area (FSC-A) measurements for forward scatter. $CD3^+$ cells were considered to correspond to singlet cells and the proliferation of $CD3^+CD4^+$ and $CD3^+CD8^+$ and CFSE-stained cells was analysed with FlowJo®. **(B)** PBMCs (250,000 cells) were labeled with CFSE and cultured in the presence of concanavalin A (ConA)

and lectin from *Phytolacca americana* (pokeweed) (PWM) for 6 days. They were then harvested and analysed in a FACSCanto machine. The red line on histograms indicates the levels of T-cell proliferation obtained in the different conditions, as determined by CFSE fluorescence loss. The black line corresponds to CFSE fluorescence in unstimulated PBMCs. Histograms show populations gated by FCS vs. SSC, singlets and the $CD3^+$ population. Representative results from two independent experiments are shown. **(C)** The graph shows the percentage of divided cells (% divided cells) in the CFSE proliferation assay for the T-cell populations gated as $CD3^+$, $CD3^+CD4^+$ and $CD3^+CD8^+$, after selection by FCS vs. SSC and singlets. **(D)** The graph shows the proliferation index in CFSE proliferation assays for T-cell populations gated as $CD3^+$, $CD3^+CD4^+$ and $CD3^+CD8^+$, after selection by FCS vs. SSC and singlets. M is his mother and F is his father. Values, (mean$\pm$SEM), were calculated from two independent experiments.

Figure S9

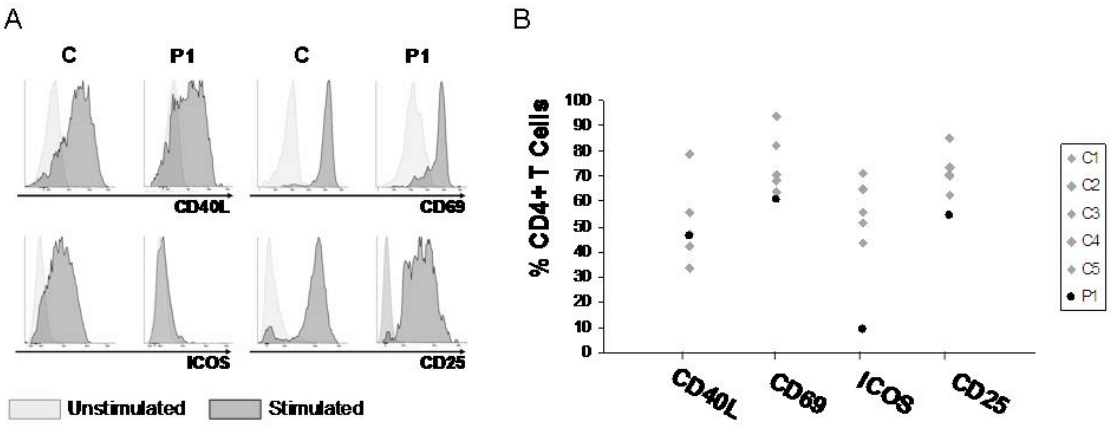

Figure S9. Response of T cells to TCR stimulation

(A) CD40L, CD69, inducible T-cell costimulator (ICOS) and CD25 expression after the CD3/CD28 stimulation of $CD4^+$ T cells. Stimulated expression of CD40L, CD69, ICOS and CD25 PE (dark gray) was compared with unstimulated expression (light gray). **(B)** Percentage of $CD4^+$ T cells positive for the indicated markers, for P1 (black circles) and five healthy controls (gray diamonds). The experiment was performed once with cells from P1.